

HARDENING-SOFTENING BEHAVIOR AND MINIMUM REINFORCEMENT OF RC BEAMS

K. Rokugo, N. Kurihara, T. Ito, Y. Uchida, and W. Koyanagi
Department of Civil Engineering, Gifu University, Gifu, Japan

Abstract

The flexural failure behavior of RC beams made of different kinds of concrete and reinforcing materials is investigated. High strength concrete (HSC), aramid fiber and steel fiber reinforced concrete (AFRC and SFRC) and continuous fiber reinforced plastic (FRP) grid are included in addition to normal strength concrete (NSC) and ordinary steel bars. The favorable failure modes of RC beams are discussed. In the case of beams reinforced with steel bars, the minimum reinforcement ratios were 0.15% for NSC beams, 0.4% for HSC beams and 1.0% for SFRC beams in the range of this study. High performance non-metallic RC beams could be produced by combining AFRC and FRP grid.

1 Introduction

Fracture Mechanics of Concrete (FMC) covers modeling of fracture behavior of concrete, numerical analysis of fracture behavior of members, applications to structural design, etc.

In addition to conventional structural design methods based on simple

equations for load and stress estimations, more accurate structural design methods based on the actual failure behavior of structural members are needed, which can be calculated through numerical analysis. For the more accurate design methods, FMC can propose constitutive models including softening region and reliable methods to calculate softening, localization and bifurcation behaviors of structures. For the conventional design methods, FMC is helpful to improve accuracy of design equations taking account of knowledge such as size effects. FMC can also give more appropriate explanations of minimum reinforcement in relation to hardening–softening behavior.

In this contribution, test results on the flexural failure behavior of RC beams made of different kinds of concrete and reinforcing materials are presented. High strength concrete (HSC), steel fiber and aramid fiber reinforced concrete (SFRC and AFRC) and continuous fiber reinforced plastic (FRP) grid are included in addition to normal strength concrete (NSC) and steel reinforcing bars. The distribution of deformation in beams in the hardening condition up to the peak load and the concentration of deformation in the softening condition after the peak load are discussed in relation to the minimum reinforcement. The favorable failure modes of RC beams are also discussed.

2 Failure mode

To discuss favorable failure modes of members, three types of load–displacement curves A, B and C of beams in flexure are illustrated in Fig. 1 [Rokugo et al. 1993]. The characteristics of curve A are superior to those of B and C in the following aspects.

- The ultimate load is the highest (large load carrying capacity).
- The displacement at the ultimate is the largest (large ductility).
- The toughness (area under curve) is the largest (high toughness).
- The initial stiffness is the largest (high stiffness).
- The curve turns at point "a" before the ultimate. This gives warning of the coming ultimate load point (warning of failure).
- The beam does not break, and consequently beam portions may not suddenly fall down (prevention of breaking).

The ultimate load and the ductility should be chosen considering the economical aspects, the balance of the performances, etc. The warning through the turning of the curve is not always necessary but is valuable in many cases. The prevention of breaking is not essential. This is not necessary when the breaking never occurs because the failure of another part precedes or when the dropping of broken portions does not

cause serious damage. Moreover, the prevention of breaking may be not easy to be achieved in the actual cases of large members because of the own weight.

In general, there are the minimum and the maximum limitations in the tension reinforcement ratios for RC beams in order that the deflection increases with a certain increase of load after the yield point to warn us of the coming ultimate. As illustrated in Fig. 2, the steel has large hardening region but the concrete in tension has little hardening region. Moreover, steel reinforcing bars have a large elongation at rupture (10% or more in Japan) and a high ratio of tensile strength to yield strength (about 1.3 in Japan). The large hardening portion of steel contributes to the dispersion of deformation (rotation at cracked regions) along the beam axis.

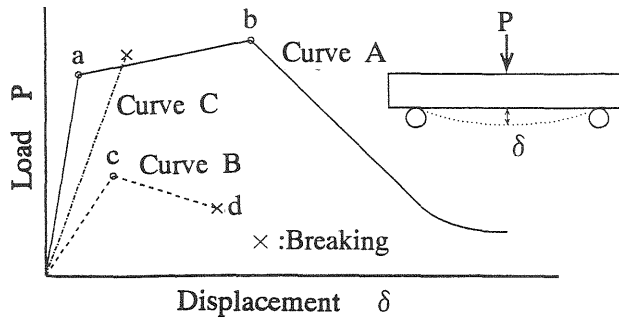


Fig. 1. Comparison of load-displacement curves

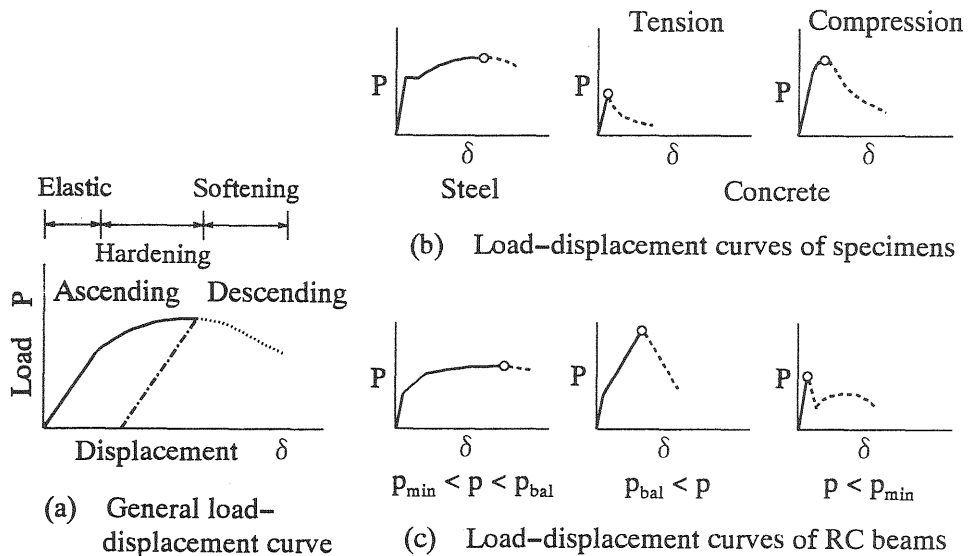


Fig. 2. Hardening and softening in load-displacement curves

3 Failure behavior of beams reinforced with FRP grid

Fiber reinforced plastic (FRP) rods and grids, which are made of continuous fibers such as aramid, carbon, glass, etc. bound with resin, have potential to be substituted for steel bars in reinforced and prestressed concrete structures. FRP rods and grids are light, strong, and free from corrosion. They are, however, brittle and have no yield point. Their elongation at rupture is small and their Young's modulus is low as compared with steel bars. FRP grids have been used, for example, instead of steel wire meshes in shotcrete.

In this chapter, the flexural failure behavior of concrete beams made of three kinds of concrete and reinforced with FRP grid is discussed.

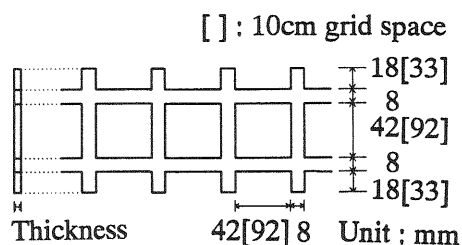


Fig. 3. Sizes of FRP grid

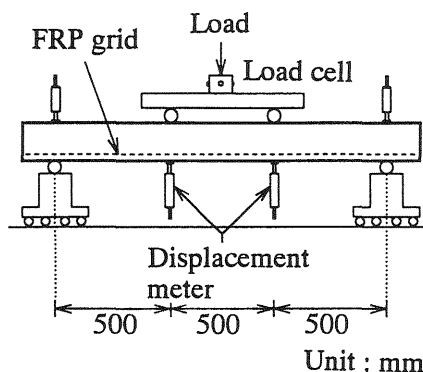


Fig. 4. Loading tests

Table 1. Test conditions of beams reinforced with FRP grid

Series	Concrete	Specimen size, mm			FRP grid	
		Width	Span [Moment span]	Depth	Bar No.	Grid space, mm
PH6 PH8 PH11 PH14 PH18	High strength concrete	100	1500 [500]	60 80 110 140 180	G4	50
PN6 PN8 PN11 PN14 PN18	Normal strength concrete	200	1500 [500]	60 80 110 140 180	G4	100
PF8 PF14 PF23	Aramid fiber rein. concrete	100	1500 [500]	80 140 230	G6	50

3.1 Experimental procedures

As indicated in Table 1, thirteen series of concrete beams (two beam specimens in each series) were made using three kinds of concrete (high strength concrete, normal strength concrete and aramid short fiber reinforced concrete (AFRC)) and FRP grid as reinforcement. The depth of beams were varied. FRP grids (bar number: G4 and G6) were made of continuous glass fibers. Their properties are given in Table 2 and their shapes are shown in Fig. 3, where the grid spaces are 50 mm or 100 mm. The thickness of cover concrete was 10 mm. Properties of three kinds of concrete are given in Table 3. Properties of aramid short fibers used in AFRC are shown in Table 4. As illustrated in Fig. 4, beam specimens were loaded at third points (moment span: 500 mm). The applied load and the displacement (deflection) at loading points were recorded.

Table 2. Properties of FRP grids

Bar No.	Tensile strength kgf/cm ²	Young's modulus kgf/cm ²	Guaranteed maximum load tonf	Sectional area mm ²	Grid space mm
G4	6000	3.0×10^5	0.78	13	50 or 100
G6	6000	3.0×10^5	2.10	35	50

Table 3. Properties of concrete including AFRC

Concrete	Strength kgf/cm ²			Young's modulus kgf/cm ²	Age at testing days
	Compression	Tension	Flexure		
High strength concrete	766	59.7	96.0	3.85×10^5	19
Normal strength concrete	327	27.4	46.4	2.94×10^5	11
Aramid fiber reinforced concrete*	801	(103)	156	3.36×10^5	23

* AFRC contains 2% of aramid short fibers

Table 4. Properties of aramid short fibers for AFRC

Size of fiber		Specific gravity	Tensile strength kgf/cm ²	Young's modulus kgf/cm ²
Diameter mm	Length mm			
0.4	30	1.39	3.0×10^4	7.0×10^5

3.2 Test results and discussions

Load–displacement curves of two beams and a crack pattern on one beam side for each series are shown in Figs. 5 to 7. FRP grids ruptured at the final stage in all beams. The number of cracks, the crack load P_{cr} (load at the first crack) and the maximum load P_u due to resistance of FRP grid are averaged from two beams and are tabulated in Table 5.

3.2.1 Behavior of beams of PH and PN series

Since the Young's modulus of FRP grids is lower and the bond with concrete is weaker than steel bars, the shapes of load–displacement curves of PH series (high strength concrete) and PN series (normal strength concrete) are like saw–teeth, where the load sudden dropped just after formations of a new crack. If the loading test is done under a load–controlled condition, the step–shaped load–displacement curves may observed as shown in Fig. 8.

When the maximum load P_u was clearly higher than the crack load P_{cr} (PH6, PH8, PN6, and PN8 series), more than 4 cracks were observed and the final displacement at rupture was larger than 40 mm. However, when P_u was lower than P_{cr} (PH14, PH18, PN14, PN18 series), only one crack developed and the final displacement was too small, even considering the effect of beam depths on the final displacement.

3.2.2 Behavior of beams of PF series

The load–displacement curves of PF series (aramid short fiber reinforced concrete) were smooth without sudden load–reductions up to the peak. In the case of PF8 series, the ratio P_u/P_{cr} was larger than three, and the final displacement was large (about 70 mm). On the hardening condition up to the peak, many cracks developed due to addition of aramid fibers. That is, the addition of aramid fibers deleted the saw–toothed behavior of beams reinforced with FRP grid. High performance non–metallic concrete beams could be produced by combining AFRC and FRP grid.

3.2.3 Crack load

The crack loads were estimated through two ways and are given in Table 5. In the estimation–1, the flexural strength of concrete, which was determined from standard flexural tests (specimen size: 100×100×400 mm), was used as usually. In the estimation–2, the effect of specimen depth was taken into account by the following equation [Uchida et al. 1992],

$$f_b / f_t = 1.0 + 1.0 / (0.85 + 4.5d / L_{ch}) \quad (1)$$

Table 5. Test results of beams reinforced with FRP grid

Series	Load at first crack, Pcr, tonf			Number of cracks	Maximum load due to FRP grid, Pu, tonf	Ultimate load per one FRP bar, tonf	$\frac{P_u}{P_{cr}}$
	Experiment	Estimation -1	Estimation -2				
PH6	0.210	0.225	0.246	7	0.341	0.842	1.62
PH8	0.355	0.396	0.413	5	0.472	0.869	1.33
PH11	0.762	0.757	0.742	1	0.777	0.983	1.02
PH14	1.22	1.26	1.18	1	1.03	0.986	0.84
PH18	1.94	2.04	1.82	1	1.38	1.03	0.71
PN6	0.243	0.195	0.213	5	0.343	0.890	1.41
PN8	0.447	0.371	0.385	4	0.510	0.915	1.14
PN11	0.727	0.661	0.652	2	0.736	0.968	1.01
PN14	1.13	1.14	1.08	1	1.01	1.01	0.89
PN18	1.76	1.94	1.74	1	1.24	0.923	0.70
PF8	0.400	0.705	-	24	1.51	2.87	3.78
PF14	1.20	2.17	-	17	3.50	3.47	2.92
PF23	2.87	5.56	-	15	6.58	3.89	2.29

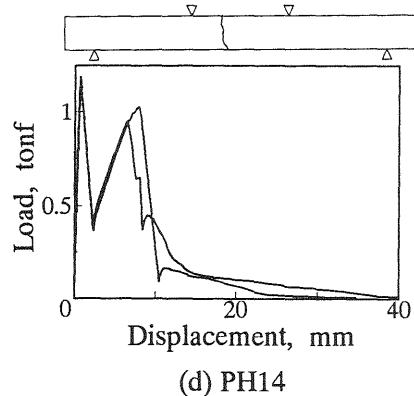
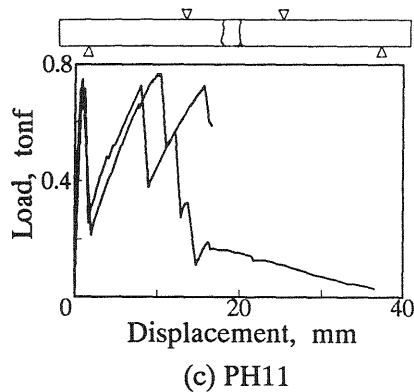
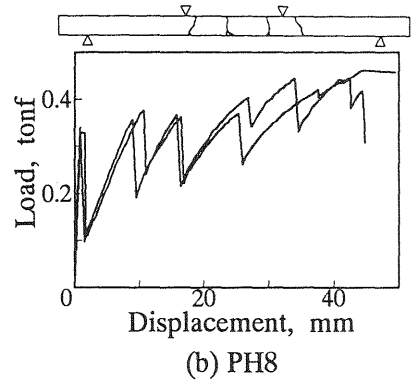
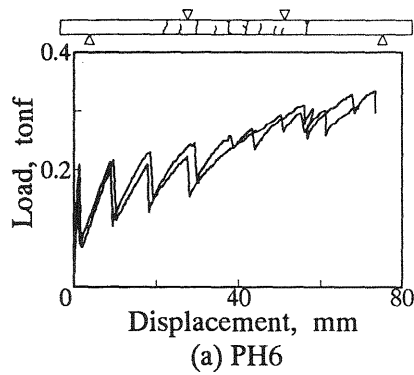


Fig. 5. Behavior of HSC beams reinforced with FRP grid (PH series)

First, the characteristic length L_{ch} was obtained from eq.(1) by putting the values of tensile strength f_t and the flexural strength f_b (the specimen depth = 100 mm) in Table 3. Then, the flexural strength of beams differing in depth d was determined from eq.(1) by using the values of L_{ch} and f_t . For PN18 series, the value of the estimation-2 was closer to the measured value than the estimation-1.

3.2.4 Ultimate tensile load of FRP grid

The FRP grid used in this study consists of two longitudinal bars. The ultimate tensile load per one FRP bar was determined from the maximum load, P_u . The rectangular stress block was taken in the compression zone of beams. As shown in Table 5, the determined ultimate load per one FRP bar exceeded the maximum value in Table 2, which were guaranteed by the manufacturer. The determined ultimate load tends to decrease with an decrease in the beam depth. The cause would be the effect of local bending deformation of FRP grids at cracked regions.

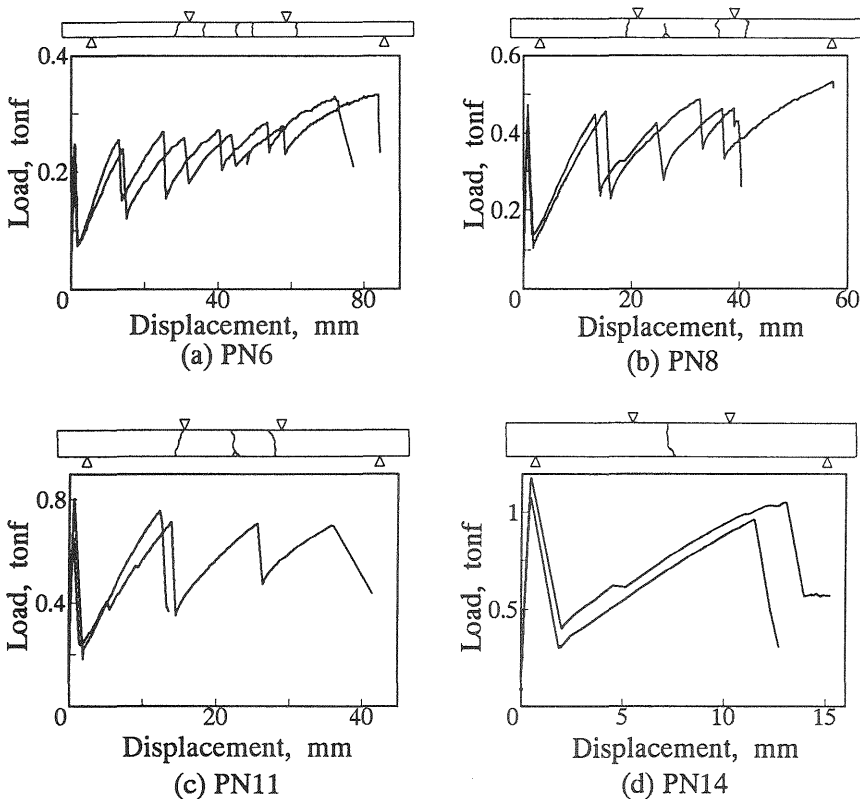


Fig. 6. Behavior of NSC beams reinforced with FRP grid (PN series)

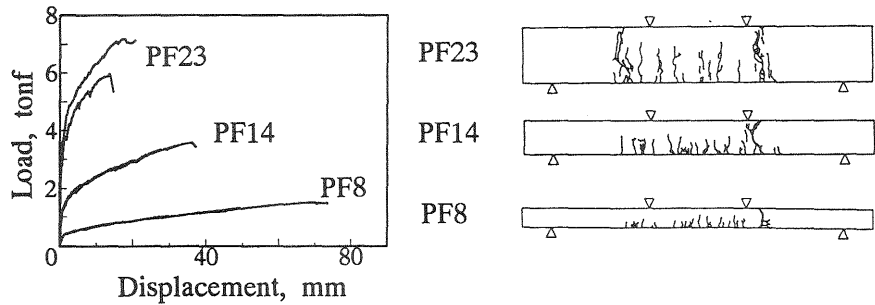


Fig. 7. Behavior of AFRC beams reinforced with FRP grid (PF series)

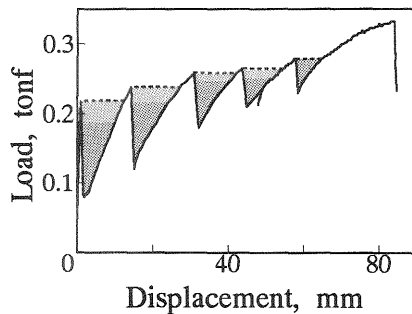


Fig. 8. Saw-toothed and step-shaped load-displacement curves

3.2.5 Minimum reinforcement for beams reinforced with FRP grid

It is seen from the results in section 3.2.1 that a large displacement accompanying plural cracks is guaranteed for beams reinforced with FRP grid when P_u/P_{cr} is greater than one. Since the sectional area of FRP grid is not so clear, the load ratio P_u/P_{cr} seems to be a more suitable index than the area ratio $p=(\text{area of reinforcement})/(\text{concrete area})$ to describe the minimum reinforcement.

Accurate estimations of P_{cr} and P_u are important to obtain reliable value of P_u/P_{cr} . The scatter of flexural strength and the effects of drying and sizes should be considered when calculating P_{cr} . In calculation of P_u , it should be noticed that the local bending decreases the strength of FRP grid. When the members are designed using the guaranteed maximum load of FRP grid, an appropriate value of P_u/P_{cr} , for example, more than 1.5, should be chosen for ductile failure.

4 Failure behavior of beams reinforced with steel bars

Flexural failure behavior of RC beams made of high strength concrete, normal strength concrete and steel fiber reinforced high strength concrete are investigated in this chapter.

4.1 Experimental procedures

Test conditions of RC beams are given in Table 6. The properties of concrete at the age of testing are shown in Table 7. SFRC contained 2% of indented steel short fibers (diameter: 0.6 mm, length: 30 mm, strength: 110 kgf/mm² (1.08 GPa)). Beams were reinforced with steel bars, D10 (diameter: 9.53 mm, yield strength: 39 kgf/mm² (382 MPa), tensile strength: 54 kgf/mm² (530 MPa)). The thickness of cover concrete was 20 mm. For SH series (high strength concrete), the beam width was changed to vary the tension reinforcement ratio. For both SN series (normal strength concrete) and SF series (steel fiber reinforced concrete), the beam depth was changed. RC beams were loaded in the same way as described in the previous chapter.

Table 6. Test conditions of RC beams

Series	Concrete	Specimen size, mm				Tension reinforcement	
		Width	Span [Moment span]	Depth	Effective depth	Bars	Ratio %
SH18 (W10)	High strength concrete	100	1500 [500]	180	155	1D10	0.46
SH18 (W14.5)		145				1D10	0.32
SH18 (W20)		200				1D10	0.23
SN14	Normal strength concrete	200	1500 [500]	140	115	1D10	0.31
SN18				180	155	1D10	0.23
SN23				230	205	1D10	0.17
SN30				300	275	1D10	0.13
SF14	Steel fiber reinforced concrete	200	1500 [500]	140	115	3D10	0.92
SF18				180	155	3D10	0.68
SF23				230	205	3D10	0.51
SF30				300	275	3D10	0.38

Table 7. Properties of concrete including SFRC

Concrete	Strength kgf/cm ²			Young's modulus kgf/cm ²	Age at testing days
	Compression	Tension	Flexure		
High strength concrete	863	88.5	54.3	4.10×10^5	24
Normal strength concrete	323	49.9	28.9	2.84×10^5	11~12
Steel fiber reinforced concrete*	888	119	89.6	4.05×10^5	22

* SFRC contains 2% of steel short fibers

4.2 Test results and discussions

Test results (average of two beams) are given in Table 8. The measured load–displacement curves are shown in Figs. 9 to 11. The load at the first crack P_{cr} (\bullet), the load at steel yielding P_y (\blacktriangle) and the maximum load due to resistance of steel bars P_u (\blacksquare) are indicated in the figures. Since the maximum loads for SF series were not clear, the loads at an inflection point were taken to be P_u for convenience.

4.2.1 Behavior of beams of SH and SN series

As seen from Fig. 9, on the load–displacement curves of SH18(W10), there were several small sharp indentations resulting from formations of new cracks. With an increase in the beam width, the crack load P_{cr} increased and the ratio P_u/P_{cr} became less than one. For SH18(W20) series, only one crack formed and the final displacement was small. For high strength concrete, the minimum reinforcement ratio for ductile behavior must be greater than 0.4% in the range of this study.

In the case of RC beams made of normal strength concrete, as seen from Fig. 10, when the tension reinforcement ratio was greater than 0.15%, plural cracks formed and the beams failed in ductile mode.

4.2.2 Behavior of beams of SF series

The load–displacement curves of beams made of steel fiber reinforced concrete (SF series) were smooth without indentations because of the fiber addition. Plural fine cracks formed during the first crack and the yielding of steel bars. After the yielding, only one main crack extended and the beam rotation concentrated at this main crack portion. It is seen from the results in this study that the tension reinforcement ratio should be greater than 1.0% in order that the ratio P_u/P_{cr} is greater than 1.0, which means plural wide cracks extend after the yielding and the final displacement becomes large.

4.2.3 Crack load of SH and SN series and yield load of SF series

The crack loads P_{cr} for SH and SN series were estimated through the two ways described in section 3.2.3 and are given in Table 8. The values of estimation–2, where the size effect of beam depth was taken into account, were closer to the values from experiments than those of estimation–1, especially for the deepest beams, SN30.

The yield loads P_y of SF series were high due to effects of steel fibers and were roughly estimated through the following equation.

$$P_y = P_{sy} + 0.7P_{cy} \quad (2)$$

where P_{sy} is the yield load due to steel bars neglecting the tensile resistance of concrete and P_{cy} is the crack load of SFRC beams

Table 8. Test results of RC beams

Series	Load at first crack, Pcr, tonf			Yield load, Py, tonf		Maximum load due to steel bars, Pu, tonf	Number of cracks	Pu / Pcr	Pu / Py
	Experiment,	Estimation -1	Estimation -2	Experiment	Estimation				
SH18 (W10)	1.94	1.94	1.72	1.75	-	2.15	3	1.11	1.23
SH18 (W14.5)	2.54	2.76	2.46	1.74	-	2.39	2	0.94	1.37
SH18 (W20)	3.53	3.88	3.46	1.79	-	2.47	1	0.70	1.38
SN14	1.22	1.29	1.21	0.98	-	1.71	5	1.40	1.74
SN18	2.02	2.15	1.92	1.72	-	2.36	4	1.17	1.37
SN23	2.63	3.43	2.93	2.30	-	3.16	3	1.20	1.37
SN30	4.82	6.06	4.92	3.43	-	4.41	1	0.91	1.29
SF14	1.96	3.15	-	5.76	5.84	(5.51)	9	(2.81)	(0.96)
SF18	3.85	5.25	-	8.17	8.70	(7.53)	8	(1.96)	(0.92)
SF23	6.27	8.39	-	11.7	12.6	(9.94)	8	(1.59)	(0.85)
SF30	9.36	14.3	-	19.0	19.1	(14.5)	9	(1.55)	(0.76)

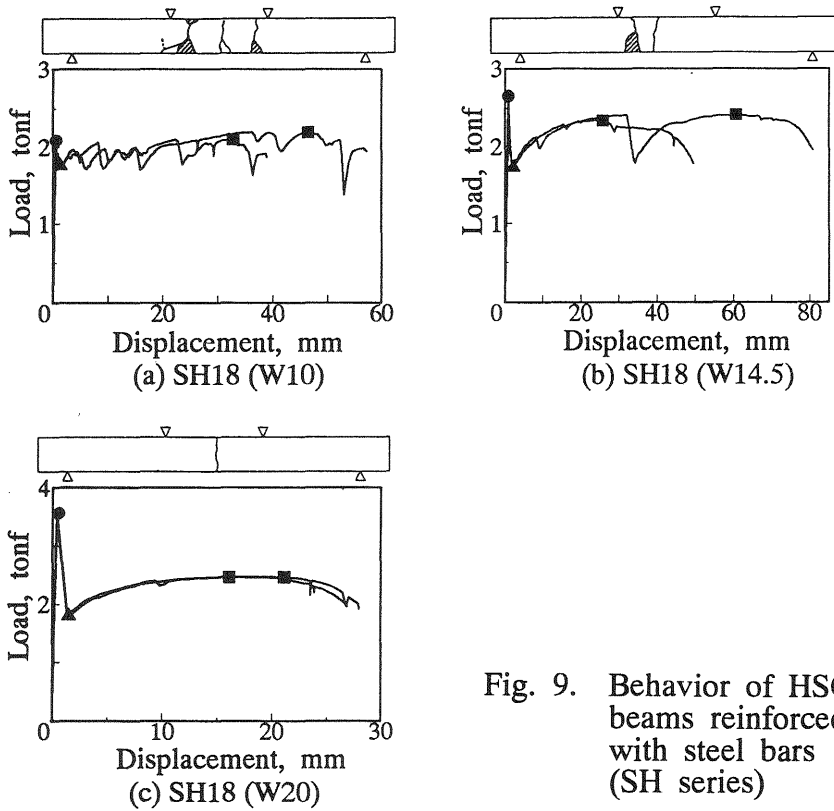


Fig. 9. Behavior of HSC beams reinforced with steel bars (SH series)

without steel bars, which is the value of estimation-1 in Table 8.

4.2.4 Minimum reinforcement for RC beams

As is known, the two conditions of $P_u > P_{cr}$ and $P_u > P_y$ must be satisfied in order that the beams behave in a ductile failure mode with

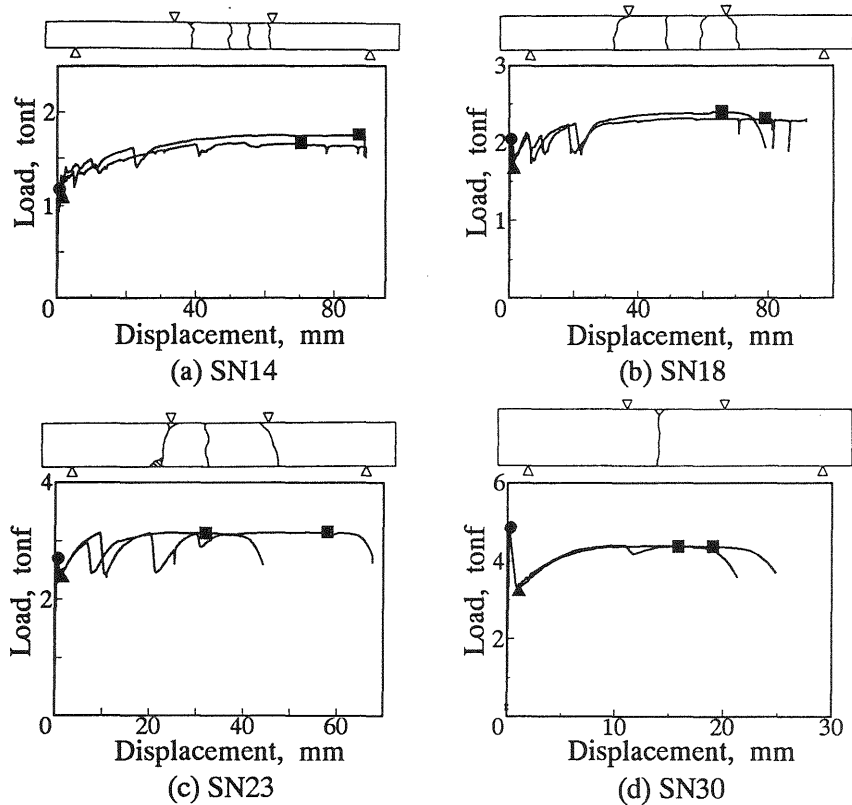


Fig. 10. Behavior of NSC beams reinforced with steel bars (SN series)

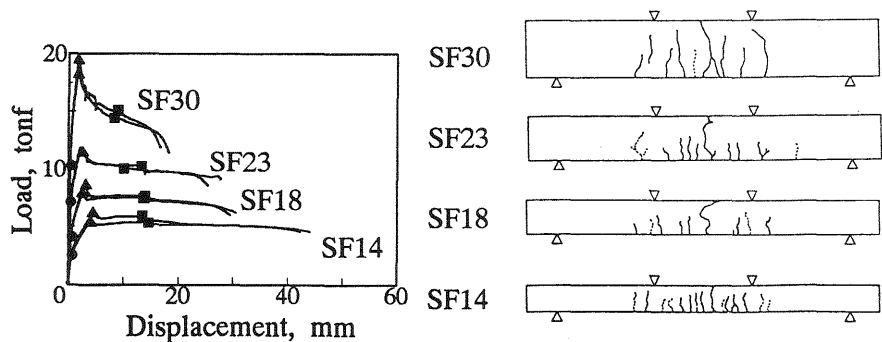


Fig. 11. Behavior of SFRC beams reinforced with steel bars (SF series)

plural wide cracks. The loads P_{cr} , P_y and P_u should be appropriately evaluated. The size effect of beam depth on the crack load P_{cr} should be taken into account for deeper beams. In the case of SFRC, the effect of steel fiber addition on the yield load P_y must be considered. The minimum reinforcement ratios for the ductile behavior were 0.15% for SN series, 0.4% for SH series and 1.0% for SF series.

5 Conclusions

The flexural failure behavior of beams made of different kinds of concrete and reinforcing materials are investigated in relation to the hardening–softening behavior and the minimum reinforcement. It is confirmed that the two conditions of $P_u > P_{cr}$ and $P_u > P_y$ must be satisfied in order that the beams fail in a ductile mode with plural cracks.

In the case of beams reinforced with FRP grid, the effect of local bending on the strength of FRP grid should be known in the evaluation of P_u . Since the sectional area of FRP grid is not so clear, the load ratio P_u/P_{cr} is more suitable than the area ratio to describe the minimum reinforcement. High performance non–metallic concrete beams could be produced by combining AFRC and FRP grid.

In the case of RC beams, the minimum reinforcement ratios for the ductile behavior were 0.15% for NSC beams, 0.4% for HSC beams and 1.0% for SFRC beams in the range of this study. For SFRC beams, in order to adequately evaluate the yield load P_y , the resistance of steel fibers must be taken into account. The size effect of beam depth on the crack load was not negligible for deeper beams.

The favorable failure modes of beams are discussed. Favorable features such as warning of failure and prevention of breaking are pointed out.

6 References

- Rokugo, K., Iwase, H., Uchida, Y. and Koyanagi, W. (1993a) Failure behavior and structural design of concrete members reinforced with continuous fiber reinforcing materials. **Proc. of Symp. on Advanced Technology on Design and Fabrication of Composite Materials and Structures, Torino**, (In press).
- Uchida, Y., Rokugo, K. and Koyanagi, W. (1992) Application of fracture mechanics to size effect on flexural strength of concrete. **Concrete Library of JSCE**, 20, 87–97.